HOSTED BY
ELSEVIER
Available online at www.sciencedirect.com
ScienceDirect
Soils and Foundations 63 (2023) 101266
SOILS AND FOUNDATIONS
www.elsevier.com/locate/sandf

Technical Report

Incorporating installation effects into the probability analysis of controlled modulus columns

Jakub Konkol

Faculty of Civil and Environmental Engineering, Department of Geotechnics and Hydraulic Engineering, Gdańsk University of Technology (GUT), Gdańsk, Poland

Received 18 March 2022; received in revised form 24 November 2022; accepted 7 December 2022

Abstract

This technical report presents the probabilistic analysis which integrates the Monte Carlo simulation (MCS) with random field theory to model the load–displacement behavior of Controlled Modulus Columns (CMCs) in overconsolidated Poznań clay. Presented study focuses on the practical aspects of statistical analysis of geotechnical data, numerical model development, and results evaluation. Variability and spatial distribution of geotechnical parameters are based directly on field and lab testing. The inherent variability of soil parameters obtained from geotechnical investigation at the site is similar to the values reported in worldwide datasets for clays. The extensive discussion about incorporation of installation effects into numerical modelling is made. It was found that proper incorporation of installation effects is governed by correct estimation of initial stress level and interface shear strength parameters. The Anisotropic Undrained Shear Strength (AUS) model which captures nonlinear behavior and anisotropy of soil (Krabbenhøft et al., 2019) is a good choice to model overconsolidated clay in intact and interface zones. The application of total stress approach, the AUS model, installation effects, and natural (inherent) variability of soil and interface parameters is sufficient to explain differences in CMC load – displacement behavior observed in the field.
© 2022 Production and hosting by Elsevier B.V. on behalf of The Japanese Geotechnical Society. This is an open access article under the CC BY-NC-ND license (http://creativecommons.org/licenses/by-nc-nd/4.0/).

Keywords: Controlled modulus columns; Installation effects; Pile-soil interface; Static loading test of pile; Probabilistic analysis; Soil variability

1. Introduction

Controlled Modulus Columns (CMC) are concrete columns (piles), formed in soil with displacement screw auger, that become common soil improvement technique (ASIRI, 2012; Basu et al., 2010; Brown, 2005). Application of full displacement auger generates significant soil displacement outward the column and changes stress state in the soil (Larisch et al., 2014; Pfeiffer and Van Impe, 1993; Slatter, 2000; Suleiman et al., 2015). All effects related to such changes in stress and displacement fields are called installation effects. Taking into consideration these effects in CMCs design is crucial for economically efficient process. However, due to soil heterogeneity, stress history, and variability of geotechnical parameters, the installation effects can significantly differ which hampers the reliability assessment. In this study, the influence of the soil spatial variability on the installation effects and CMC performance under static loading test (SLT) is shown. The application of spatial variability of soil parameters in intact and interface zone around the CMC well explains the observed differences in bearing capacities of CMCs at construction field. Finally, this study shows that probabilistic analysis which integrates the Monte Carlo simulation with spatial field theory is a good tool to model load displacement behavior of CMCs.

Peer review under responsibility of The Japanese Geotechnical Society.
E-mail address: jakub.konkol@pg.edu.pl

https://doi.org/10.1016/j.sandf.2022.101266
0038-0806/© 2022 Production and hosting by Elsevier B.V. on behalf of The Japanese Geotechnical Society.
This is an open access article under the CC BY-NC-ND license (http://creativecommons.org/licenses/by-nc-nd/4.0/).

1.1. Installation effects

Installation effects are general terms related to all physical and mechanical phenomena which result from pile insertion into the soil and influence the pile bearing capacity. Installation effects are induced by displacement-type pile installation and following neighbouring soil consolidation and aging (Komurka et al., 2003). The first one who recognized the increasing pile capacity with time was Wendel (1900). In next decades, the installation effects problem was refined by other researchers (e.g., Bond and Jardine, 1991; Cummings et al., 1950; Randolph et al., 1979). The engineering aspect of the installation effects incorporation in pile designing is associated with possibility of more precise pile bearing capacity calculation. This is important factor for pile industry that allows to reduce total pile length and to lower investment costs. In the last decades, many field studies with highly instrumented piles (usually jacked steel piles) have been carried out to measure excess pore water pressures and radial stresses during the pile installation and following soil consolidation. These include the tests performed by Norwegian Geotechnical Institute (Karlsrud, 2012), Imperial College London (Bond and Jardine, 1991; Lehane and Jardine, 1994a, 1994b) and other research teams (e.g., McCabe and Lehane, 2006; Pestana et al., 2002). In terms of CMCs, the installation effects are not widely investigated. The pore water pressure and radial stress changes in soft silt were measured by Suleiman et al. (2015). The change in excess pore water pressures in organic silt during CMCs installation and pile loading was measured by Bałachowski and Konkol (2021). The pore water pressure measurement and radial stress changes assessment were done by Larisch (2014) and Larisch et al. (2014) for different types of screw displacement augers. Nguyen at al. (2019, 2017) conducted numerical study of CMCs installation sequence in layered clay. Hird et al. (2011) investigated deformation field produced by installation of screw displacement augers in clay.

1.2. Reliability-based design

Soil is statistical homogenous medium described by inherent spatial variable parameters (Hight and Leroueil, 2003; Mitchell and Soga, 2005; Phoon and Kulhawy, 1996; Uzielli et al., 2006; VanMarcke, 1983). The effects of variable geotechnical parameters are incorporated in probabilistic analysis or reliability based design (RBD) and Finite Elements Methods (FEM) using random field theory (e.g., Fenton and Griffiths, 2003; Griffiths and Fenton, 2004; Kawa et al., 2021, 2019; Kawa and Puła, 2020; Puła and Różański, 2012). Probabilistic analysis aims to determine probability of failure for pre-defined design, while RBD aims for the optimal design with prescribed failure probability (e.g., Honjo et al., 2010). To achieve above goals, the Monte Carlo simulation is usually used (Wang and Cao, 2015; Zhang et al., 2012). In terms of piles, some probabilistic analysis or RBD was previously done. For instance, Wang and Cao (2013) showed pile RBD in layered ϕ-c soil (ϕ = angle of internal friction; c = cohesion). Yang and Liang (2006) incorporated set up effects in RBD of driven piles. Tang and Phoon (2018) investigated axially loaded driven piles and calibrated resistance factors. Stuedlein et al. (2012) presented RBD of auger cast-in place piles in granular soils. Reddy and Stuedlein (2017) developed lower-bound design lines for auger cast-in place piles using RBD and SLT databases.

1.3. Aims of this research

This technical report starts with presentation of construction site in Poznań, variation of geotechnical parameters, CMCs construction details, and summary of conducted SLTs. Then, the probabilistic undrained total modeling of SLT for single CMC is presented. Incorporation of the installation effects in the interface zone is shown, and the model parameters sensitivity is studied. The probability analysis results are compared with field SLTs, and the load–displacement curves are investigated in particular. There are several research aims for this paper: (1) presentation of the inherent variability and spatial distribution of geotechnical parameters for Poznań clay; (2) simple incorporation of the installation effects in stochastic FEM analysis; (3) presentation of the probability analysis of single CMC under SLT with incorporated installation effects; (4) indication of parameters sensitivity in SLT probabilistic modeling; (5) verification of the Anisotropic Undrained Shear Strength (AUS) model (Krabbenhøft et al., 2019) effectiveness for CMC load–displacement prediction; (6) verification of the proposed methodology by comparison of probabilistic analysis with high quality SLT at Poznań site. Finally, some conclusions and recommendation related to soil parameters variability and model performance are given.

2. Poznań testing site

2.1. General site characterization

The construction site of approx. 100 000 m^2 was located in Poznań, Poland, see Fig. 1. The CMCs were basic soil improvement technology applied at the site and totally over 8700 CMCs were constructed. The subsoil consists of so-called Poznań clay. It is neogene clay that occupies vast area in central and south-western Poland. It consists of three sedimentation zones: grey clay (the oldest level), green clay, and red clay (also called fiery clay – the youngest level) (Dyjor, 1992, 1970). In Pleistocen, the Poznań clay was overloaded by glaciers, which is the main reason of overconsolidation. The CMCs at Poznań site were constructed in the upper part of red clay deposit which was formed 5.4 $\sim$ 4 mln years BP (Czapowski and Kasiński, 2002). The sixteen CMCs were proof tested (fourteen under compression load and 2 under tension load). The geologi-

MOST WIEDZY Downloaded from mostwiedzy.pl

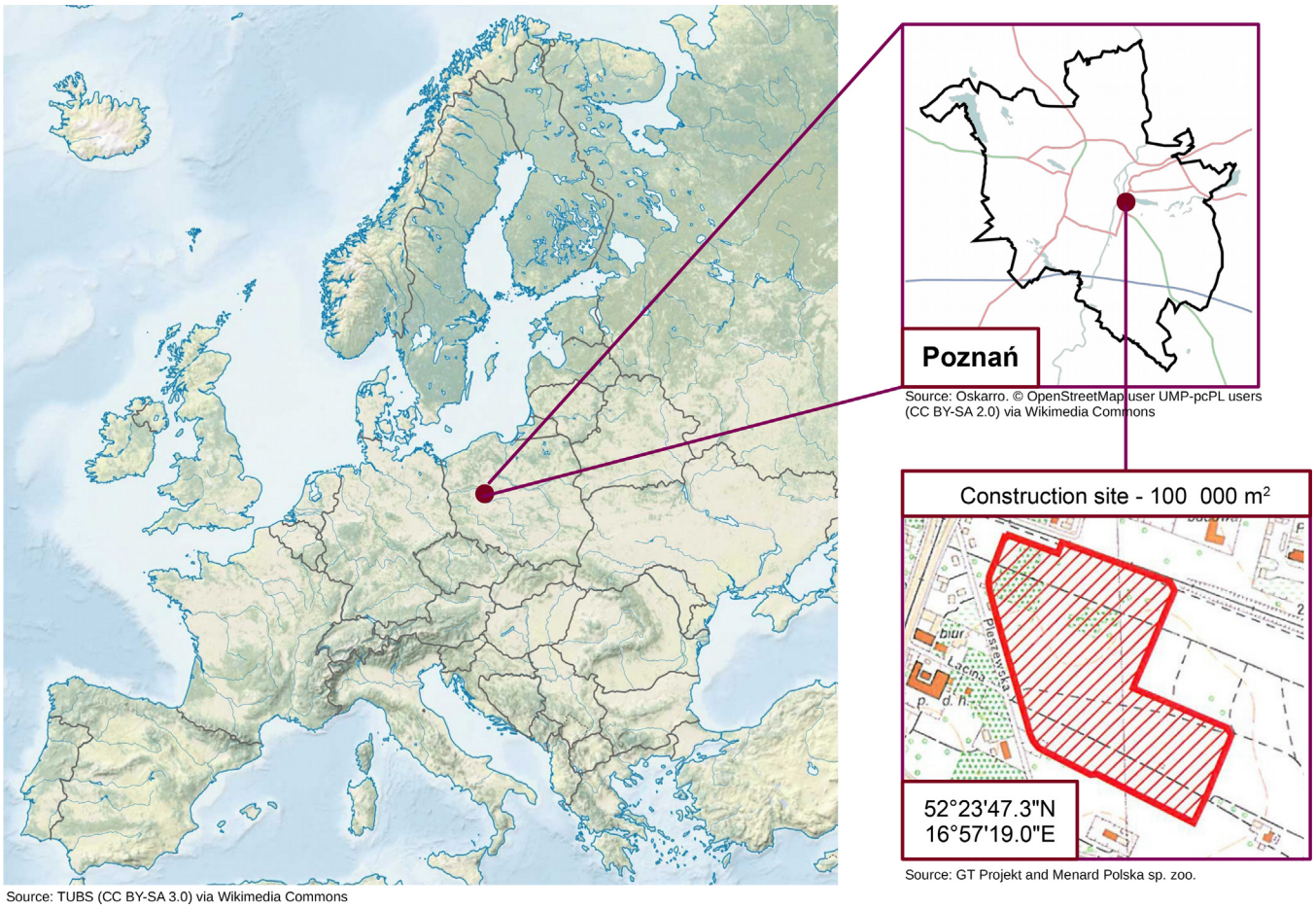

Fig. 1. Poznań testing site.

cal investigation consists of three campaigns of field and lab testing conducted in 2008, 2011 and 2012, respectively.

2.2. Controlled modulus columns

The CMCs at Poznań site have diameter of 400 mm or 360 mm and length between 6 and 11 m. In this research, dataset of eight CMCs with extensive field and lab geotechnical investigation, and high quality of SLT is under consideration. Selection of the CMCs was related to the same diameter (360 mm), similar lengths (about 7.0 m), the same SLT loading procedure, and uniform soil conditions around the columns. General information about columns is provided in Table 1. The soil profile and hydrogeological conditions around the CMCs are presented in Fig. 2. The CMCs were constructed from shallow excavation of approx. 3 m deep. As one can see, all CMCs are embedded in almost one clay layer (red Poznań clay). The upper layer (denoted as siCl) contains a little more sediment material (usually silt) than deeper layer (Cl). In two profiles (no 4 and no 5), thin delamination of sandy clay (saCl) was found. Despite such small discrepancies, uniform soil conditions for the CMCs can be recognized. The results of SLTs in terms of load-settlement curves (Q-s curve, where Q = load, s = settlement) are presented in Fig. 3. The SLTs were conducted according to method B (maintained load test) as refereed in ASTM D1143 (2020). The eight steps of loading were applied and each load increment was maintained until stabilization (0.25 mm/h). The average loading rate during SLT was around 0.04 mm/min (which corresponds to strain rate of 0.7 %/h when normalized with CMC diameter). Firstly, one can notice almost similar CMCs response in low settlement range (up to 2 ~ 3 mm). Next, the results start to differentiate. The small differences between pile lengths seem to be irrelevant, e.g., CMC no 2 (L = 6.1 m) and CMC no 6 (L = 7.0 m) have similar capacity. The time elapsed to SLT (see Table 1) seems to be also negligible in terms of axial capacity, e.g., CMC no 7 (SLT after 17 days) and CMCs no 6 and no 2 (SLT after 42 and 51 days, respectively) have similar capacities. Thus, the natural variability of soil parameters seems to be governing factor of differences in load-settlement behavior. The summary of field and lab investigations associated with each column is presented in Table 2.

MOST WIEDZY Downloaded from mostwiedzy.pl

Table 1
CMC basic information.

No	Symbol	z_{head}	z_{base}	D	L	L/D	Time to SLT	Q_{SLT}
–	–	m	m	m	m	–	days	kN
1	SD4	2,5	10,1	0,36	7,6	21,3	21	980
2	137	3,0	9,1	0,36	6,1	17,0	51	768
3	E407	3,0	10	0,36	7,0	19,4	31	937
4	H151	3,5	10,8	0,36	7,3	20,3	43	1081
5	G415	3,5	10,7	0,36	7,2	20	28	987
6	100	3,0	10	0,36	7,0	19,4	42	718
7	359	2,5	9,5	0,36	7,0	19,4	17	684
8	D689	3,5	9,6	0,36	6,1	17,0	41	581

Note: z_{head} = depth of CMC head below initial ground level; z_{base} = depth of CMC base below initial ground level; D = CMC dimeter; L = CMC length; SLT = static loading test; Q_{SLT} = CMC axial capacity estimation form SLT based on Chin (1970) extrapolation corresponding to CMC head settlement of 10 %.

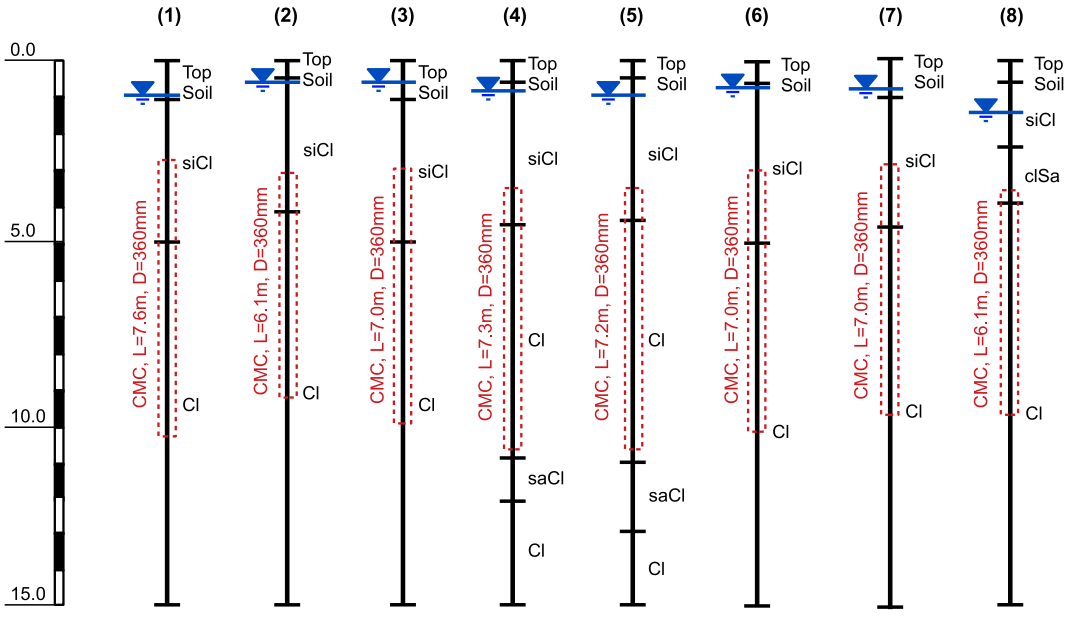

Fig. 2. Soil profiles for selected CMCs.

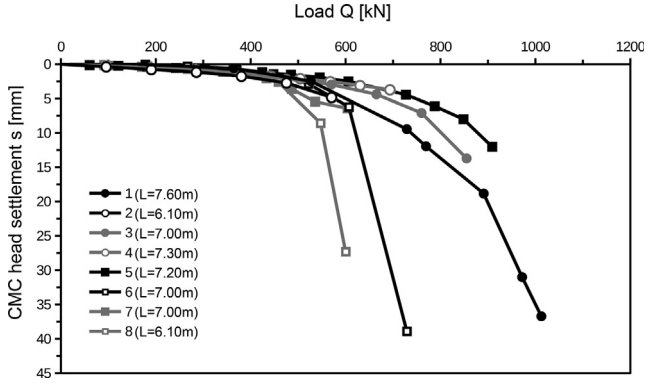

Fig. 3. CMCs load-settlement curves.

2.3. Field investigations results

Field investigation at the Poznań site consists of piezocone soundings (CPTU), flat dilatometer soundings (DMT) and borings. Fig. 4 presents the results of eight CPTU soundings in the closest distance to the investigated CMCs (totally, the 54 CPTU soundings with 22 dissipation tests were made). Corrected cone resistance (q_t) measurement increases quite linearly with depth with only single deviations produced by stiffer stratifications. The similar trend is observed for sleeve friction (f_s). Pore water pressure measurement at shoulder filter location (u_2) is quite variable due to overconsolidated nature of Poznań clay.

Fig. 5 shows the DMT results. The DMT investigation at the Poznań site consist of total five DMTs, while only three soundings were made in close vicinity of tested CMCs. All three tests show similar values of material index (I_D), dilatometer modulus (E_D) and horizontal stress index (K_D).

2.4. Poznań clay geotechnical parameters and their variability

2.4.1. Physical parameters

Wide spectrum of geotechnical investigation at the Poznań site allows for good description of parameters variabil-

MOST WIEDZY Downloaded from mostwiedzy.pl

Table 2
Field and lab tests associated with CMCs.

No	Symbol	CPTU	DISS	DMT	boring	TX	OED	PHYS	
-	-	-	-	-	-	-	-	w	ρ
1	SD4	Yes	–	Yes	Yes	–	–	Yes	Yes
2	137	Yes	Yes	–	Yes	–	–	Yes	–
3	E407	Yes	Yes	Yes	Yes	Yes	Yes	Yes	Yes
4	H151	Yes	Yes	–	Yes	–	–	Yes	–
5	G415	Yes	Yes	–	Yes	–	–	Yes	–
6	100	Yes	Yes	Yes	Yes	Yes	Yes	Yes	Yes
7	359	Yes	–	–	Yes	–	–	Yes	–
8	D689	Yes	Yes	–	Yes	–	–	Yes	–

Note: CPTU = piezocone penetration test; DISS = CPTU dissipation test; DMT = flat dilatometer test; TX = triaxial test; OED = oedometer test; PHYS = physical properties measured during lab tests; w = water content; ρ = soil total density.

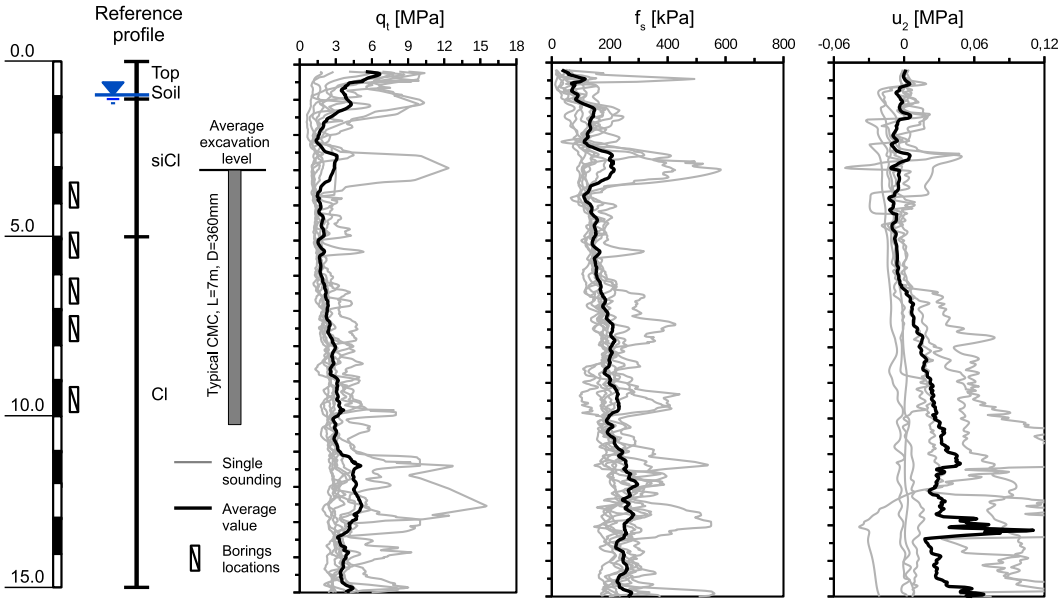

Fig. 4. CPTU testing results for selected CMCs.

ity around the CMCs. Fig. 6 presents the water content, unit weight and initial void ratio distributions along typical CMC (D = 0.36 m and L = 7.0 m) at the site. The results show quite homogenous medium. The average water content is AVG = 23.7 % (AVG = average value) with COV = 19.1 % (COV = coefficient of variation). The unit weight of 20.6 kN/m^3 is burdened with a very low variability (COV = 1.8 %). The void ratio is also in very narrow range of variability. The specific gravity was not tested, but literature data of Poznań clay (e.g., Stróżyk, 2015) indicates values between 2.68 and 2.72.

2.4.2. Overconsolidation ratio (OCR) and earth pressure at rest coefficient (K_0)

Poznań clay is moderate to highly overconsolidated soil (Kotowski and Kraiński, 1998). The OCR distributions related to CPTU, DMT and oedometer estimates are presented in Fig. 7. The CPTU-based OCR was determined using following formula (Kulhawy and Mayne, 1990):

$$OCR = 0.33\left(\frac{q_{t-\sigma_{v0}}}{\sigma\prime_{v0}}\right) \quad (1)$$

where: OCR = overcosolidation ratio; q_t = corrected cone resistance; σ_{v0} = total vertical stress; σ'_{v0} = effective vertical stress.

The DMT-based OCR estimate uses Marchetti (1980) equation:

$$OCR = (0.5K_D)^{1.56} \quad (2)$$

where: K_D = horizontal stress index.

Oedoemter estimate of OCR is determined with Casagrande method (1936). The preconsolidation pressures (σ'_c) obtained from oedometer testing are between 457 and 887 kPa, which confirms previous studies (Stróżyk, 2015). The average OCR oscillates between 5 and 10 from CPTU tests, between 5 and 10 from oedometer tests, and between 10 and 15 from DMT tests, see Fig. 7. The earth pressure at rest coefficient (K_0) related to CPTU and DMT estimates is

MOST WIEDZY Downloaded from mostwiedzy.pl

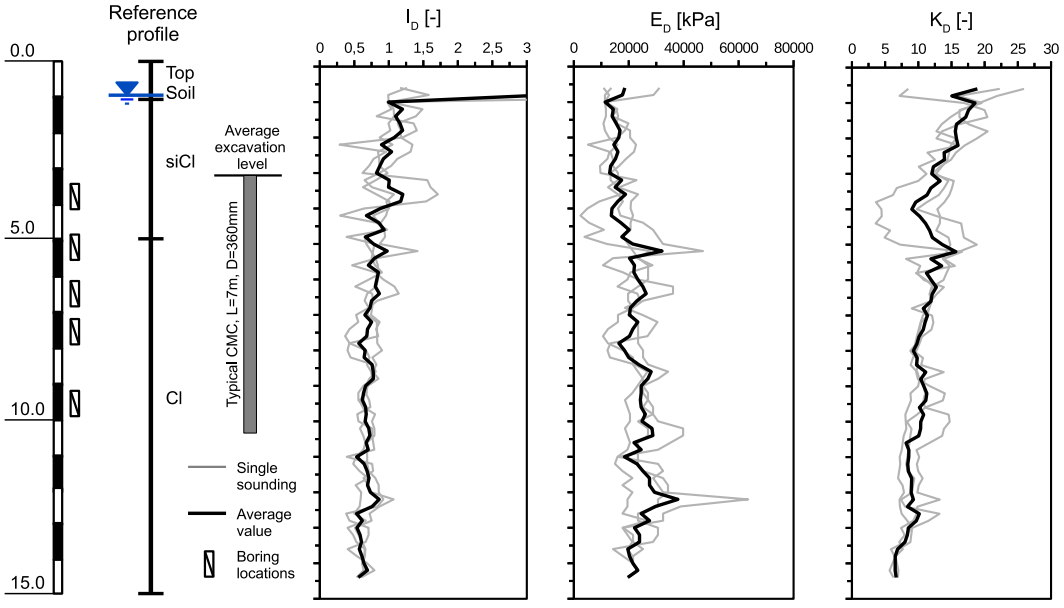

Fig. 5. DMT testing results for selected CMCs.

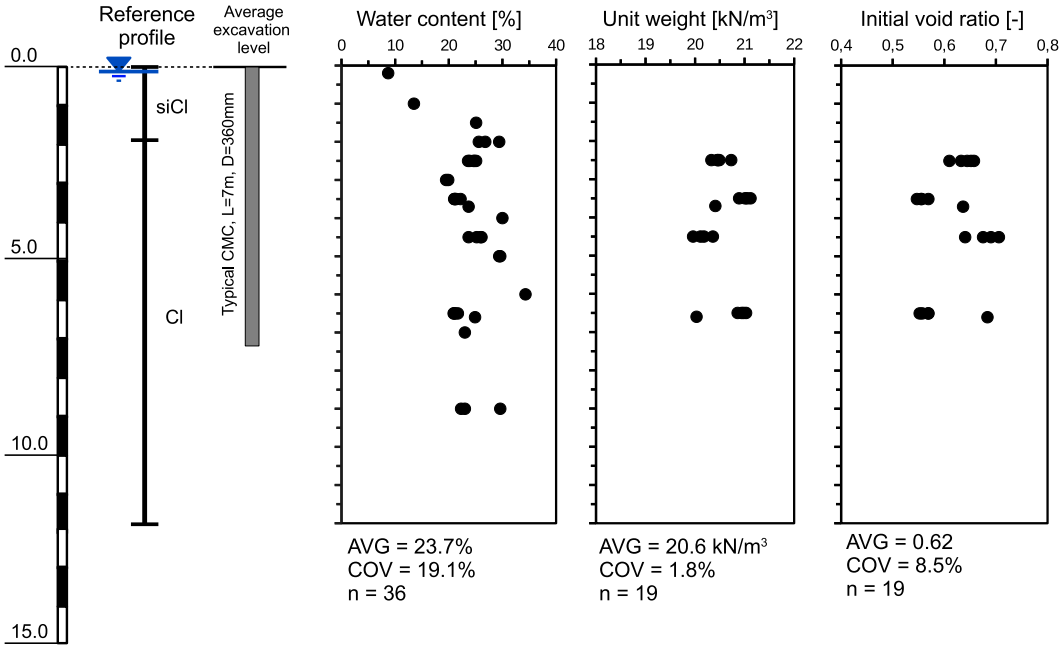

Fig. 6. Physical parameters variability along CMC at Poznań site.

shown in Fig. 8. The CPTU-based K_0 was determined using Kulhawy and Mayne (1990) proposition:

$$K_0 = 0.1\left(\frac{q_{t-\sigma_{v0}}}{\sigma\prime_{v0}}\right) \tag{3}$$

The DMT-based K_0 estimate uses Marchetti (1980) formula:

$$K_0 = (K_D/1.5)^{0.47} - 0.6 \tag{4}$$

The earth pressure at rest coefficient is quite constant along CMC shaft, see Fig. 8, and it is close to 2.

2.4.3. Total stress analysis parameters

Undrained shear strength (c_u) of soil is parameter influenced by rate of loading, anisotropy, loading history and mode of shear (Ladd and DeGroot, 2003). The CPTU-based and DMT-based correlations generally provide c_u for average mode of shear and loading rate of 1 %/h, which is typical in consolidated undrained triaxial testing (Kulhawy and Mayne, 1990). Rate of 1 %/h is also close to the value obtained during SLTs. The SHANSEP (Stress History and Normalized Soil Engineering Parameters) method allows for c_u estimation regarding mode of shear

MOST WIEDZY Downloaded from mostwiedzy.pl

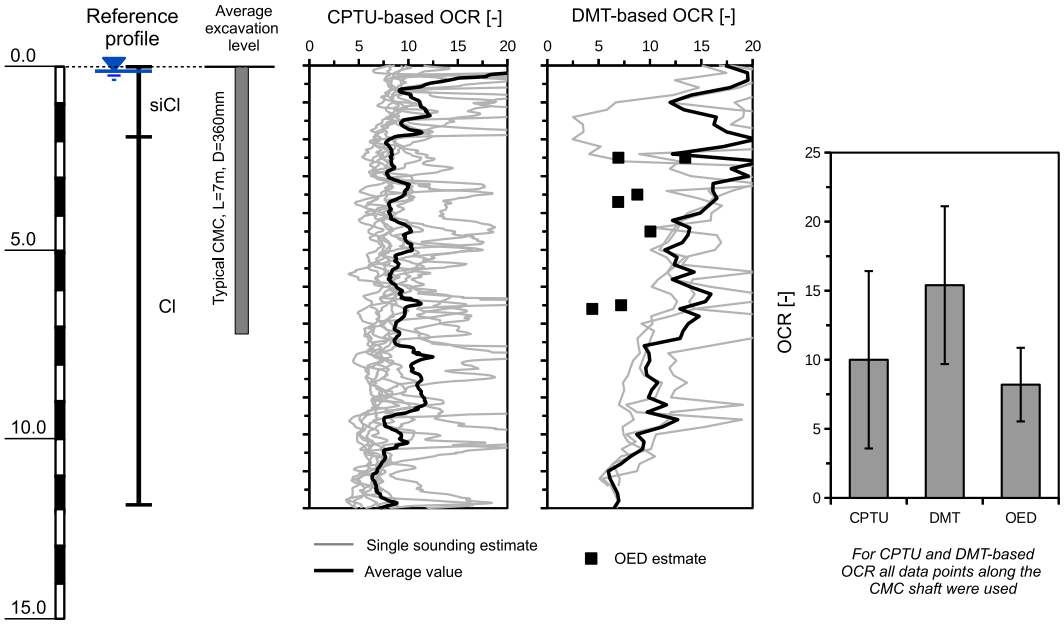

Fig. 7. OCR profiles and variability for Poznań site.

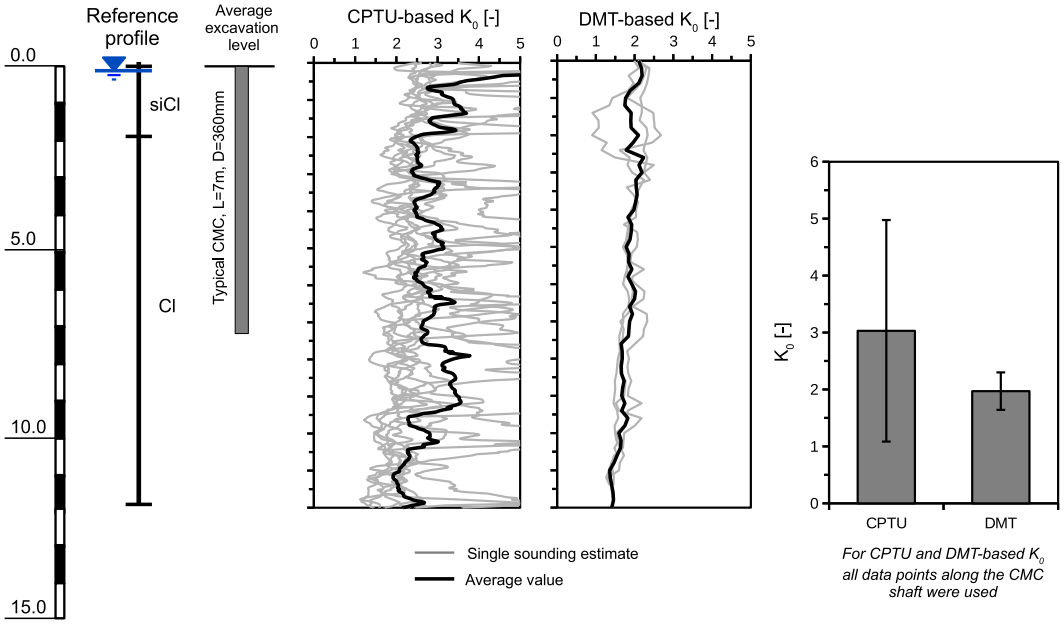

Fig. 8. K_0 profiles and variability for Poznań site.

with reference loading rate close to 1 %/h (Ladd, 1991). Fig. 9 presents the c_u estimates for Poznań clay. Both CPTU and DMT methods present linear increase of c_u with depth. The CPTU-based trend indicates $c_u = 120 + 10z$ (where z = depth below pile head). The lower bound is $c_u = 43 + 10.5z$, while the upper bound is $c_u = 197 + 10.5z$. The DMT-based trend indicates $c_u = 109 + 7z$ (lower bound: $c_u = 78 + 7.7z$; upper bound: $143 + 6z$). Due to large scatter of c_u, engineering judgment suggests that reasonable assumption is $c_u = 100 + 10z$ (see Fig. 9). The triaxial test's results and the SHANSEP estimates indicate constant values, but they can be influenced by sampling techniques and specimen quality (e.g., Zapata-Medina et al., 2014). However, these values are still in range of field estimates. Finally, the CMCs were constructed from shallow excavation. This usually induces decrease of c_u for soft soils (Yannie, 2012). However, for highly overconsolidated soils (such as Poznań clay) this effect is usually marginal (Mitachi and Kitago, 1976) and was also omitted in this research.

Fig. 10 shows the initial undrained elastic modulus (E_{u0}) change with effective mean stress obtained from Consoli-

MOST WIEDZY Downloaded from mostwiedzy.pl

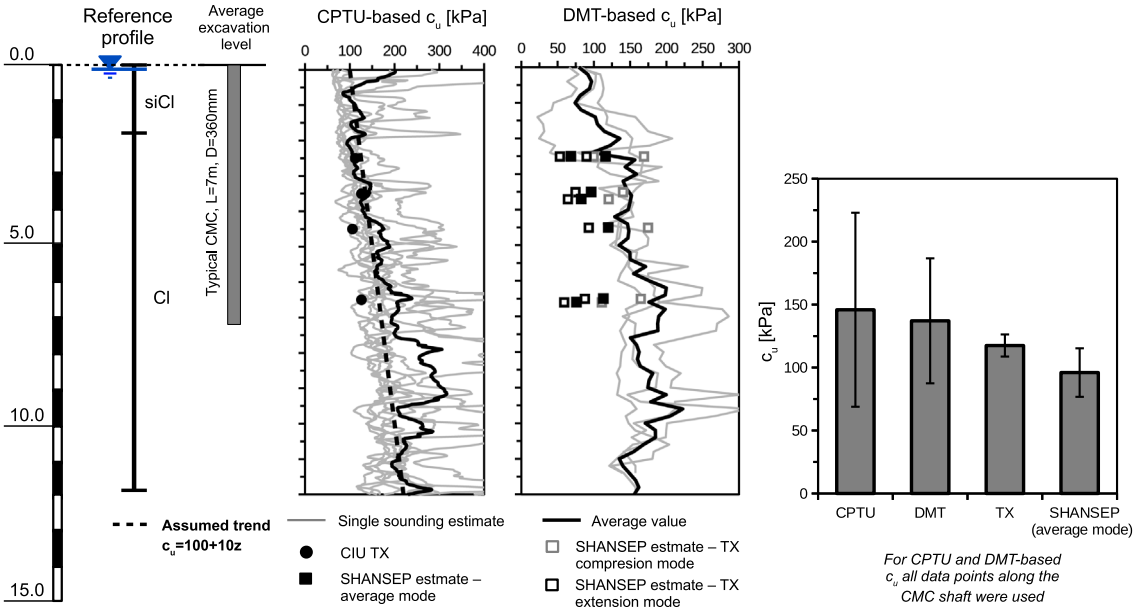

Fig. 9. Undrained shear strength profiles and variability for Poznań site.

dated Isotopically Undrained Compression (CIUC) triaxial tests (TX). The results are quite variable which is typical for overconsolidated soils and previous findings for Poznań clays (Stróżyk and Tankiewicz, 2016).

2.4.4. Effective stress parameters

Effective stress parameters will be only briefly summarized in this paragraph, as the effective stress analysis is out of scope of this paper. The average value of critical effective angle of internal friction is 15.7 ° with standard deviation SD = 1.8 ° resulting in COV = 11 % (n = 9, where n = number of measurements). The stress ratio M (for p'-q plane according to Cambridge notation, where q = deviator stress, p' = effective mean stress) is 0.60 with SD = 0.07 (COV = 12 %, n = 9). The compression index C_c is 0.073 with COV = 21 % (n = 7) and the swelling index C_s is 0.043 with COV = 33 % (n = 7).

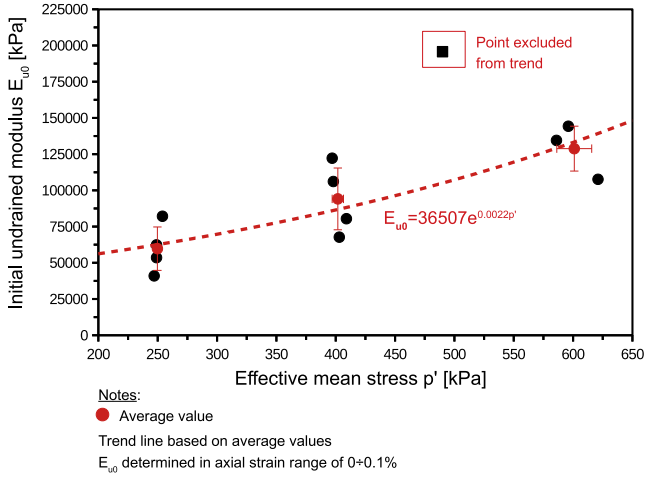

Fig. 10. Initial undrained modulus change with effective mean stress (one point was excluded from the trend due to significant deviation from the rest of data).

3. Probabilistic analysis and FEM modelling

Probabilistic analysis requires a specification of random variable (also called mean or average), its variability in terms of standard deviation (SD) or coefficient of variation (COV), type of probability distribution, and parameters of spatial distribution (also called scales of fluctuation). Some of parameters can be used directly from results of field and lab testing. Some quantities have to be however calculated from other parameters, e.g., assessment of the installation effects, described later. To do so, one have to introduce error propagation formulas (Ku, 1966), see Table 3. These formulas allow to calculate SD for more sophisticated quantities used in probabilistic FEM model.

The direct Monte Carlo Simulation (MCS) was used in this research. The soils parameters are generated using the Karhunen–Loeve expansion method which provides ana-

Table 3
Error propagation (Ku, 1966).

Function	Standard deviation
f = aA	$\sigma_f = \lvert a\rvert\sigma_A$
f = $aA + bB$	$\sigma_f = \sqrt{a^2\sigma_A^2 + b^2\sigma_B^2 + 2ab\sigma_{AB}}$
f = aA-bB	$\sigma_f = \sqrt{a^2\sigma_A^2 + b^2\sigma_B^2 - 2ab\sigma_{AB}}$
f = AB	$\sigma_f \approx \lvert f\rvert\sqrt{(\sigma_A/A)^2 + (\sigma_B/B)^2 + 2\sigma_{AB}/(AB)}$
f = A/B	$\sigma_f \approx \lvert f\rvert\sqrt{(\sigma_A/A)^2 + (\sigma_B/B)^2 - 2\sigma_{AB}/(AB)}$
f = aA^b	$\sigma_f \approx \lvert fb\sigma_A/A\rvert$
f = $a\sin(bA)$	$\sigma_f \approx \lvert ab\cos(bA)\sigma_A\rvert$
f = $a\tan(bA)$	$\sigma_f \approx \lvert ab\sec^2(bA)\sigma_A\rvert$

Note: a, b = constants; A, B = field variables, σ_A = standard deviation of A; σ_B = standard deviation of B; σ_{AB} = covariance between A and B (when the variables A and B are uncorrelated $\sigma_{AB} = 0$).

MOST WIEDZY Downloaded from mostwiedzy.pl

lytical solution for exponential covariance function (e.g., Fenton and Griffiths, 2008; Krabbenhøft et al., 2016). The basic assumption of the Karhunen–Loeve expansion method, as implemented in OPTUM (Huang et al., 2013), will be briefly described below. The covariance function C_X (**s**, **t**), where **s**, **t** ϵ D (physical space) describes how random variables vary spatially. Using Mercer's Theorem, C_X (**s**, **t**) can be decomposed to:

$$C_X(\mathbf{s},\mathbf{t}) = \sum_{i=1}^{n} \lambda_i f_i(\mathbf{s}) f_i(\mathbf{t}) \tag{5}$$

where: λ_i = eigenvalue of C_X (**s**, **t**); and $f_i(\mathbf{t})$, $f_i(\mathbf{s})$ = eigenfunctions of C_X (**s**, **t**).

Eq. (5) has to be truncated in finite number of terms and thus, the covariance will be reduced. To control the such a reduction, the eigenvalues are sorted in decreasing order and the number of terms is chosen to satisfied condition:

$$\frac{\lambda_k}{\lambda_1} \leq 10^{-5} \tag{6}$$

where: λ_1 = first (the highest) eigenvalue, λ_k = last (the lowest) eigenvalue, k = number of terms. Based on analysis for two-dimensional scenario presented by Huang et al. (2013), number of terms is set to 1000 to satisfy above condition.

Reproducibility of the Monte Carlo simulation is governed by seed number which ensures a particular, repeatable sequence (MSC run). The presented stochastic analysis contains n_{sim}-number (n_{sim} = number of simulations) of deterministic, independent simulations. The parameters used in the probabilistic model are not interrelated (e.g., c_u is not related to E_{u0}, so the same E_{u0}/c_u ratio is not preserved in each MCS run). Spatial variation of the geotechnical parameters is included in numerical model by random fields generation and series of MCS runs. The log-normal distribution is selected as a probability distribution function (PDF) for the field variables. The log-normal distribution is a simple nonlinear transformation of Gaussian normal distribution and allows for always positive random variables (e.g., Krabbenhøft et al., 2016). The log-normal PDF is described by equation:

$$f(x,\mu,\sigma) = \frac{1}{x\sigma\sqrt{2\pi}} \exp\left[\frac{-(\ln x - \mu)^2}{2\sigma^2}\right] \tag{7}$$

where: x = variable; μ and σ are model parameters related to mean (AVG) and standard deviation (SD):

$$AVG = \exp\left(\mu + \frac{\sigma^2}{2}\right) \tag{8}$$

$$SD = \exp\left(\mu + \frac{\sigma^2}{2}\right)\sqrt{\exp(\sigma^2) - 1} \tag{9}$$

The key points of spatial field generations are vertical and horizontal correlation lengths that vary depending on soil parameters. For instance, Phoon and Kulhawy (1999) suggest the vertical scale of fluctuation (CL_v) of 1 ∼ 6 m and horizontal scale of fluctuation (CL_h) of 45 ∼ 60 m. For Poznań site, the scales of fluctuation were calculated on the basis of CPTU soundings using rule of thumb method (Spry et al., 1988). It was found that CL_v = 0.44 ∼ 0.8 m while CL_h = 54 ∼ 164 m. In this research, CL_v = 0.5 m and CL_h = 60 m are used (they are lower bands of calculated fluctuation scales).

Number of MCS runs usually ranges between 1000 and 10,000 (Mooney, 1997). However, some studies show that as small values as 100 ∼ 200 runs can be also sufficient (Lerche and Mudford, 2005). Reducing number of runs is beneficial as it results in reduction of computational costs. Generally, the number of simulations is proportional to $1/p_f$ (where p_f = probability of failure). The COV of MCS can be calculated as (Au and Wang, 2014):

$$COV_{MCS} = \sqrt{\frac{1 - p_f}{n_{sim} p_f}} \tag{10}$$

where: COV_{MCS} = coefficient of variation of Monte Carlo simulation; n_{sim} = number of runs, and p_f = probability of failure. Eq. (10) can be rearranged to following form:

$$n_{sim} = \frac{1}{(COV_{MCS})^2} \frac{1 - p_f}{p_f} \tag{11}$$

Using very low value of COV_{MSC} and p_f (e.g., COV_{MSC} = 0.1 and p_f = 0.01) one get n_{sim} = 9900 runs. Consequently, the number of runs should be close to 10 000 and such a value was used in this research. Eq. (10) can be also used in analysis of probabilistic model to calculate probability of failure, when COV_{MCS} will be known. This topic will be further covered in conclusion section.

3.1. General concept

Nonlinearity and anisotropy are the key features of overconsolidated Poznań clay. The reference SLTs took few hours to complete enforcing undrained conditions. Thus, the total stress analysis was selected for numerical analysis. The Anisotropic Undrained Shear Strength Model (AUS) developed by Krabbenhøft et al. (2019) was used as a constitutive model. The AUS model allows to capture stress and fabric anisotropy as well as strength nonlinearity. The parameters for the model can be determined from standard lab tests, see Table 4.

Numerical model consists of soil domain divided into two parts: (1) interface region, where installation effects will be included, and (2) intact soil region, where installation effects can be neglected. The pile will be assumed as rigid due to significant differences in stiffness between pile and soil, lack of stiff layer under the pile toe, typical pile length/diameter ratio and low expected axial forces (up to 1000 kN). Pile can be modelled also as a perfectly elastic material (E = 30GPa and ν = 0.15, where E = Young modulus and ν = Poisson ratio), but the differences in this particular case are negligible.

MOST WIEDZY Downloaded from mostwiedzy.pl

Table 4
The AUS model parameters.

Parameter	Description	Tests
–	–	
E_{u0}	Initial undrained modulus	CIUC or CK_0UC
ν_u	Undrained Poisson's ratio, equal to 0.49	N/A
c_u^c	Undrained shear strength in triaxial compression mode	CIUC or CK_0UC
c_u^e/c_u^c	Ratio of undrained shear stress anisotropy	CIUC or CK_0UC (CIUE or CK_0UE is not necessary as c_u^e/c_u^c is related to angle of internal friction)
$\varepsilon_{c,50}$	Axial strains corresponding to half of the maximum deviator in triaxial compression mode	CIUC or CK_0UC
$\varepsilon_{e,50}$	Axial strains corresponding to half of the maximum deviator in triaxial extension mode	CIUE or CK_0UE
K	Total stress ratio	DMT or CPTU
γ	Soil total unit weight	LAB

Note: CIUC = consolidated isotopically undrained compression; CK_0UC = consolidated K_0 undrained compression; CIUE = consolidated isotopically undrained extension; CK_0UE = consolidated K_0 undrained extension; LAB = lab determination; DMT = flat dilatometer test; CPTU = piezocone penetration test; N/A = not applicable.

The probabilistic FEM model of CMC static loading test consists of axisymmetric domain, see Fig. 11, and 10 000 Monte Carlo runs. In each run, the multiplier load acting on the pile head is increased in ten steps. Five steps are related to "elastic" response of the model and following five steps to "plastic" response. The advantage of such a strategy is smooth load-settlement curve. The disadvantage is lack of maximum displacement of 0.1D (10 % of CMC diameter) in every MCS run due to occurrence of plastic deformation at small displacements (which strictly depends on random field generation and parameters values). The calculations were conducted in OptumG2 software suit using Gaussian 6-node triangular elements. The mesh of 200 elements was refined from the boundaries towards the pile. The smallest elements of 0.06 m were located near pile base and soil surface. The preliminary tests involving other elements and mesh sizes were conducted. The difference between Gaussian 6-node element and most accurate Gaussian 15-node element was about 1.6 %. The difference between model containing 200 elements (smallest element of 0.06 m) and 2000 elements (smallest element of 0.006 m) was 3.2 %. Consequently, the proposed mesh size, element number, and element type are good suited to provide computation accuracy and effectiveness in MCS involving 10 000 runs.

3.2. Parameters sensitivity

Sensitivity studies show how model is sensitive to each parameter and allow to optimize numerical solution. The sensitivity analysis was performed on the average values of geotechnical parameters. The results are summarized in Table 5. For considered case and loading scheme, the E_{u0}, c_u^c and $\varepsilon_{c,50}$ are highly important in the interface zone. Outside the interface, the influence of the E_{u0}, c_u^c and $\varepsilon_{c,50}$ is very limited. This is not surprising, as interface parameters governs the shaft behavior. However, under the CMC base, the intact soil parameters were of great importance. The influence of stress anisotropy was generally very limited. The displacement of the CMC head of 36 mm (10 % of CMC diameter) did not enforce negative deviator stress in soil domain. In base area, the deviator stress was significantly lowered, but still positive. Consequently, for Poznań clay parameters and applied loading scheme, no extension mode in the model was encountered. The influence of initial stress ratio was very limited. The K value was important to provide initial stress state in the soil but during analysis its influence on results was negligible. This is consistent with theoretical background of total stress analysis. The pile rigidity (perfectly rigid or perfectly elastic with E = 30GPa and $\nu = 0.15$) is also of low influence on results.

Another aspect of the sensitivity study was pile length. In the field, the CMCs lengths vary from 6.1 to 7.6 m, but probabilistic model will only cover 7.0 m pile. The difference in CMC lengths results in capacity difference of about 10 %. The calculated capacity was 10.8 % lower for 6.1 m CMC (the shortest CMC), and 8.3 % higher for 7.6 m CMC (the longest CMC), in comparison with CMC of 7.0 m. These values are in range of assumed COV_{MCS} = 10 %. Thus, the direct comparison of MCS results and field data is acceptable.

3.3. Intact soil region

The soil parameters and their variability, see Table 6, were obtained directly from lab and field tests described previously. The undrained strength was assumed to linearly change with depth with COV = 25 %. Such value represents satisfactory field and lab measurements described previously, see Fig. 9. The E_{u0} with COV = 20 % was estimated using TX results (Fig. 10). The c_u^e/c_u^c ratio is established with a following formula (Krabbenhoft and Lyamin, 2015):

$$\frac{c_u^e}{c_u^c} = \frac{3 - \sin\phi\prime}{3 + \sin\phi\prime} \tag{12}$$

MOST WIEDZY Downloaded from mostwiedzy.pl

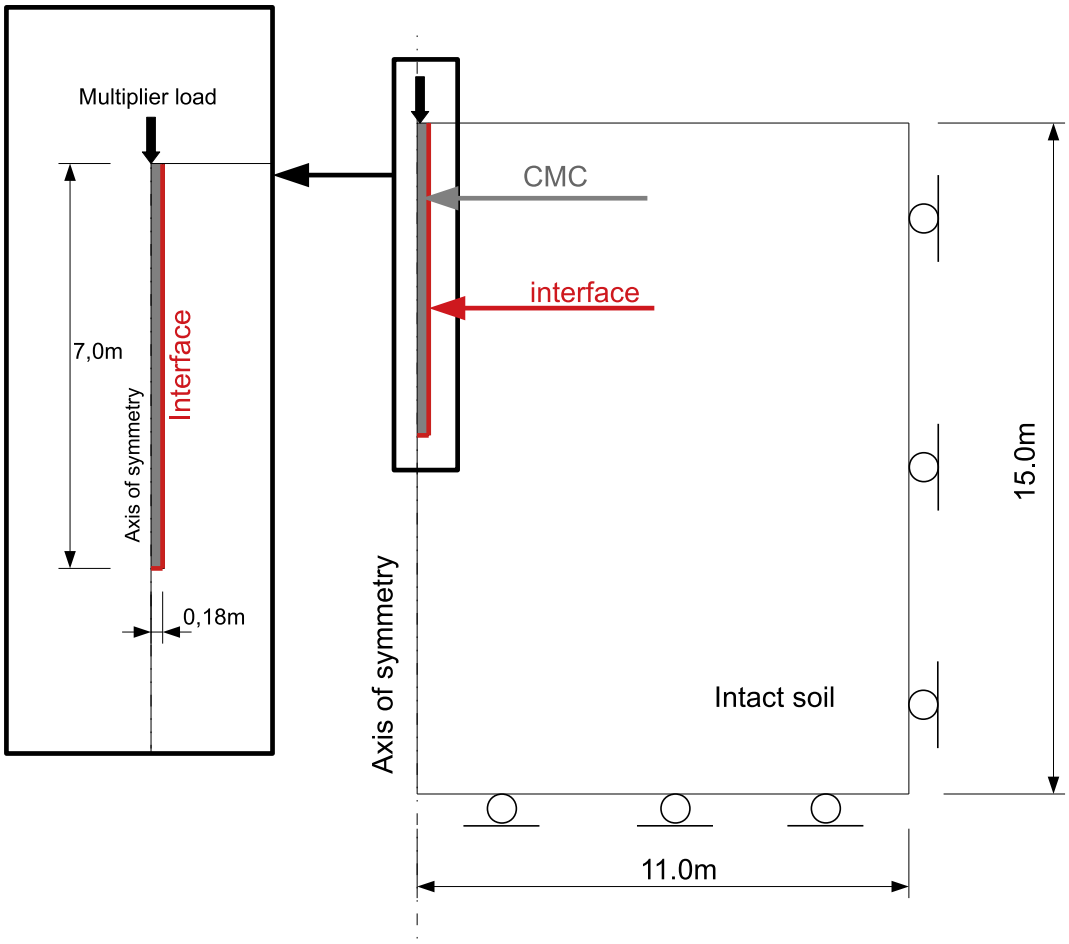

Fig. 11. FEM model of CMC SLT for probabilistic analysis.

Table 5
The AUS parameters sensitivity in numerical model.

Parameter	Interface zone	Intact soil
–	–	
E_{u0}	high	v. low at the shaft; high under pile base
c_u^c	high	v. low at the shaft; high under pile base
c_u^e/c_u^c	v. low	v. low
$\varepsilon_{c,50}$	high	v. low at the shaft; high under pile base
$\varepsilon_{e,50}$	v. low	v. low
K	v. low	v. low

Note: E_{u0} = Initial undrained modulus; c_u^c = Undrained shear strength in triaxial compression mode; c_u^e/c_u^c = Ratio of undrained shear stress anisotropy; $\varepsilon_{c,50}$ = Axial strains corresponding to half of the maximum deviator in triaxial compression mode; $\varepsilon_{e,50}$ = Axial strains corresponding to half of the maximum deviator in triaxial extension mode; K = Total stress ratio.

where: c_u^e = undrained shear strength in triaxial extension test; c_u^c = undrained shear strength in triaxial compression test; ϕ' = effective angle of internal friction.

Table 6
The AUS model parameters for intact soil and interface zone.

Parameter	Intact zone		Interface zone	
–	AVG	COV	AVG	COV
E_{u0} [MPa]	41.4	20 %	59.7	20 %
ν_u [-]	0.49	–	0.49	–
c_u^c [kPa]	100 + 10z	25 %	95	30 %
c_u^e/c_u^c [-]	0.75	5 %	0.75	5 %
$\varepsilon_{c,50}$ [%]	0.4	45 %	0.4	45 %
$\varepsilon_{e,50}$ [%]	0.4	45 %	0.4	45 %
K [-]	1.5	30 %	5.2	30 %
γ [kN/m^3]	20.6	5 %	20.6	5 %

Note: E_{u0} = Initial undrained modulus; ν_u = undrained Poisson's ratio c_u^c = Undrained shear strength in triaxial compression mode; z = depth below CMC head level; c_u^e/c_u^c = Ratio of undrained shear stress anisotropy; $\varepsilon_{c,50}$ = Axial strains corresponding to half of the maximum deviator in triaxial compression mode; $\varepsilon_{e,50}$ = Axial strains corresponding to half of the maximum deviator in triaxial extension mode; K = total stress ratio (for interface zone $K = K_c^{tot}$); γ = soil total unit weight.

Eq. (12) returns $c_u^e/c_u^c = 0.83$ with COV = 1.2 %. The alternative estimate is $c_{ue}/c_{uc} = 0.5 + 0.0034PI$, where PI = plasticity index (Ladd, 1991). It results in $c_u^e/c_u^c = 0.64 \sim 0.69$. Finally, the $c_u^e/c_u^c = 0.75$ with COV = 5 % was assumed. It is average from TX and SHANSEP esti-

MOST WIEDZY Downloaded from mostwiedzy.pl

mates. The $\varepsilon_{c,50} = 0.4$ % with COV = 45 % is based on TX data. The $\varepsilon_{e,50}$ is the only parameter that have to be assessed due to lack of lab testing. However, the sensitivity study showed negligible influence of this parameter. The $\varepsilon_{e,50} = \varepsilon_{c,50}$ is used, which is quite common for overconsolidated soils (e.g., Zhu and Yin, 2000). The $\varepsilon_{e,50}$ for soft soils is usually few times higher than $\varepsilon_{c,50}$ (e.g., Won, 2013). To determine initial stress state, $K_0 = 2.0$ with COV = 20 %, see Fig. 8, was used. The switch from K_0 to K can be done with equation:

$$K = \frac{\sigma_{h0}}{\sigma_{v0}} = \frac{K_0\sigma\prime_{v0} + u_0}{\sigma\prime_{v0} + u_0} \tag{13}$$

where: K = total stress ratio; σ_{h0} = initial horizontal total stress; σ_{v0} = initial vertical total stress; K_0 = earth pressure at rest coefficient; σ'_{v0} = initial vertical effective stress; u_0 = hydrostatic pressure.

Eq. (13) returns K = 1.5 with COV = 30 %. The AUS model response in triaxial compression mode (for average parameters) in comparison to the lab tests is shown in Fig. 12. The differences in initial part of the q-ε curve are related to "pure elastic" behavior (defined by E_{u0} and $\varepsilon_{c,50}$).

3.4. Interface zone

Parameters in the interface zone can be quite different in relation to those in the intact zone. Several studies showed that installation of displacement pile increases horizontal stress and changes soil strength parameters around the pile (Bond and Jardine, 1991; Gavin et al., 2008; Karlsrud, 2012). Such increase of horizontal stresses usually overloads the soil and induces increase in undrained shear strength. Below, some further considerations are provided.

3.4.1. Randolph et al. (1979)

Since CMCs were installed using a displacement auger, it is reasonable to use installation effects formulas that originate from the Cavity Expansion Method (CEM). Consequently, according to Randolph et al. (1979) the final undrained shear strength in vicinity of the pile can be estimated as:

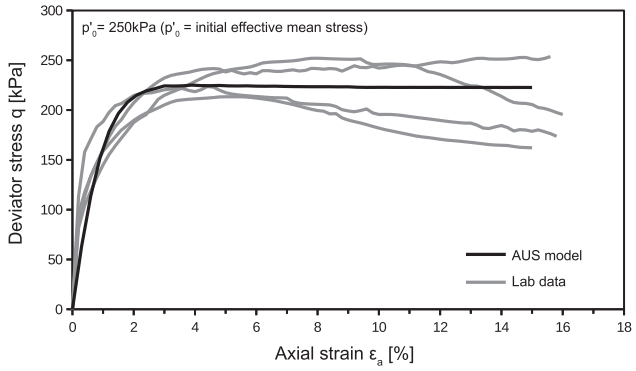

Fig. 12. The AUS model performance versus lab tests.

$$c_u(\infty) = \frac{c_u(0)}{\sigma'_c}\left(\frac{\sqrt{3}}{M} + 3\right)c_u(0) \tag{14}$$

where: $c_u(\infty)$ = undrained shear strength after pile installation and subsequent soil consolidation, $c_u(0)$ = initial undrained shear strength; σ'_c = preconsolidation pressure; M = stress ratio in p'-q plane (Cambridge notation).

The disadvantage of Eq. (14) is necessity of selection of adhesion factor (α) to calculate interface shear failure stress (undrained interface strength). The adhesion factor can range between 0.4 and 1.0 depending on initial stress state, plasticity index and interface type (e.g., Doherty and Gavin, 2011). For Poznań clay, the average parameters along the pile shaft are: $c_u(0) = 120 \pm 30$ kPa, $\sigma'_c = 670 \pm 167.5$ kPa, and $M = 0.60 \pm 0.07$. Consequently, the $c_u(\infty) = 127 \pm 56$ kPa (COV = 44 %). The $c_u(\infty)$ is higher than $c_u(0)$ and burdened with high uncertainty due to error propagation functions and parameters with high COV ($c_u(0)$ and σ'_c). Furthermore, one should apply adhesion factor to calculate interface failure stress. For Poznań clay, $\alpha = 0.3 \sim 0.7$ depending on code or design practice (e.g., American Petroleum Institute, 2000; Kulhawy, 1991; Tomlinson and Woodward, 2015), which can produce even larger uncertainty in the interface failure stress ($\alpha c_u(\infty)$). For instance, $\alpha = 0.5 \pm 0.2$ results in $\alpha c_u(\infty) = 63.5 \pm 37.6$ kPa (COV = 59 %) Consequently, the application of Eq. (14) for Poznań clay site is rather limited. However, it can be successfully applied in normally consolidated (NC) soils, where, for instance, study by Li et al. (2019) revealed that $c_u(\infty)$ after installation and soil consolidation was about $1.2c_u(0)$.

3.4.2. Konkol (2017)

Konkol (2017) introduces the installation effects coefficient (IEC) based on the high quality dataset of instrumented piles to estimate effective horizontal stress acting on the pile shaft:

$$\sigma\prime_{h,eq} = IEC\left[\left(\frac{\sqrt{3}}{M} + 1\right)c_u(0) + \sigma'_{v0}\right] \tag{15}$$

where: IEC = installation effect coefficient, $IEC = 0.26OCR^{0.41}$; σ'_{v0} = initial vertical effective stress.

Although Eq. (15) is an effective stress approach, it can be used to determined directly $\alpha c_u(\infty)$, see Fig. 13. For concrete piles, the interface friction angle (δ) is usually similar to the effective angle of internal friction (ϕ') (e.g., Chen et al., 2015; Di Donna et al., 2016). Application of the average parameters along the pile shaft ($M = 0.6 \pm 0.07$, $c_u(0) = 120 \pm 30$ kPa and $OCR = 10 \pm 3$) and error propagation functions (Table 3) returns the average $\sigma'_{h,eq} = 338 \pm 93$ kPa, which corresponds to $K_c = 9.1 \pm 2.5$ (K_c = effective stress ratio after pile installation and soil consolidation) and $K_c^{tot} = 5.2 \pm 1.5$ (K_c^{tot} = total stress ratio after pile installation and soil consolidation). Such a high horizontal stress are in range of reported data, see section 3.4.3. Significant overload of soil at the interface enforces

MOST WIEDZY Downloaded from mostwiedzy.pl

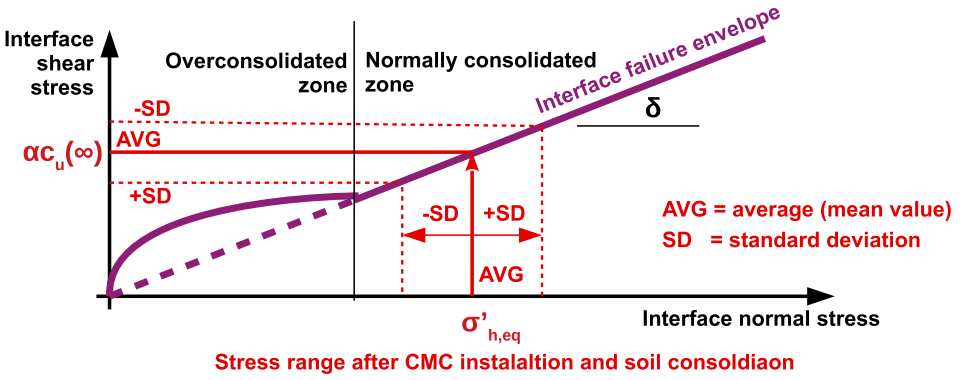

Fig. 13. Effective approach model for undrained shear strength of interface determination.

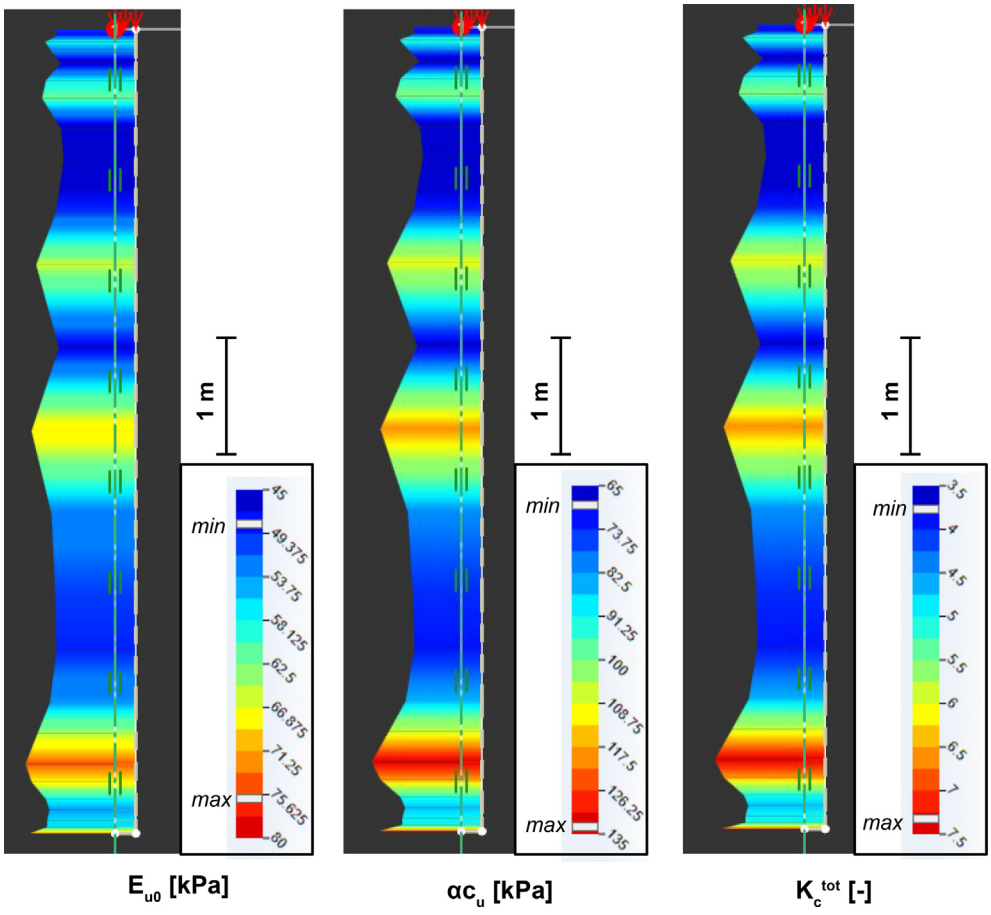

Fig. 14. Strength parameters and stress ratio variability in interface zone in probabilistic analysis (100th run).

the soil behavior in normally consolidated range during SLT. Using $\delta = \phi$', the interface failure shear stress is $\alpha c_u(-\infty) = 95 \pm 28$ kPa (COV = 30 %). In the probabilistic FEM model of CMC static loading test, above estimate and the AUS model were chosen to model interface behavior. The E_{u0} was estimated using a CIUC trend line (Fig. 10) with COV = 20 % based on TX data. The $\varepsilon_{c,50} = -\varepsilon_{e50}$ are the same as for the intact soil. Using the same or very similar values of E_{u0}, $\varepsilon_{50,c}$ and $\varepsilon_{50,e}$ for the intact soil and the rough interface is convenient and supported by various research (e.g. Chen et al., 2015) as long as similar testing conditions (i.e., proper mean stress, shearing rate) are maintained.

3.4.3. Other estimates

Previous research also provides some guidelines about effective stress ratio K_c. For instance, Karlsrud (2012) provided $K_c = 0.5 \sim 1.5$ for lightly overconsolidated soils and $K_c = 1.4 \sim 4.0$ for highly overconsolidated soils. For highly overconsolidated London clay (Bond and Jardine, 1991), K_c varies between 6 and 8. Gavin et al. (2008) reports $K_c = 2 \sim 8$ depending on pile installation technology. Xu

MOST WIEDZY Downloaded from mostwiedzy.pl

et al. (2006) find value of $K_c = (1.5 \sim 4)K_0$ for normally consolidated soft soils. The $K_c = 1 \sim 2$ was found by Suleiman (2015) for CMCs in soft, plastic silt. Well-established value of $K_c = 1.0\ K_0$ (Meyerhof, 1976) for stiff, overconsolidated clays is used in codes and design practice (e.g., Brown et al., 2010, 2018). In most of the referred research, the K_c varies along the pile shaft and is the highest near the pile base (e.g., Bond and Jardine, 1991; McCabe and Lehane, 2006). Based on above findings, the proper (or average) value of K_c can be hampered to determine. The general trend suggests lower values of K_c for lightly overconsolidated soils and higher K_c for highly overconsolidated soil.

4. Results and discussion

4.1. Random field generation

The random field generation of geotechnical parameters is shown for 100th run of MCS as an example. Fig. 14 presents variability of the E_{u0}, αc_u and K_c^{tot} at the interface, and Fig. 15 shows field of the E_{u0}, c_u in intact zone. As one can see, the variability is moderate and reflects the field and lab measurements. The variability distribution is consistent with used scales of fluctuations. The similar distributions (shapes) of field variables is consequence of the same spatial field generated for each MCS run.

4.2. SLT probabilistic analysis

The comparison between load-settlement curves measured in the field and the ones from probabilistic analysis is presented in Fig. 16a (standard, linear scale presentation) and Fig. 16b (log-scale presentation). Log-scale presentation allows for more details insight into the settlement behavior. As can be seen, most of the MCS runs slightly overestimate settlement in small settlement range (up to 3 mm). It is result of 'pure elastic': behavior of Poznań clay in very small strain range and possible underestimation of E_{u0}. It also results from the AUS model, where E_{u0} and $\varepsilon_{c,50}$ defines initial part of the q-ε curve. Similar fitting problem was encountered in TX modeling, see Fig. 12. The rest of the Q-s curves ($3 \sim 36$ mm) are within the range of the field data. The axial capacities of CMC are presented in Fig. 17. As one can see, the most of SLT capacities are in the same range as the values from stochastic FEM.

The last covered aspects are the standard error (SE), COV_{MSC} and p_f. Fig. 18 presents the SE with confidence level of 95 %, p_f, and COV_{MSC}. For more than 1000 runs, COV_{MSC} is about 12 %, which is very close to the initially assumed value of 10 %. The calculated (from Eq.(10))

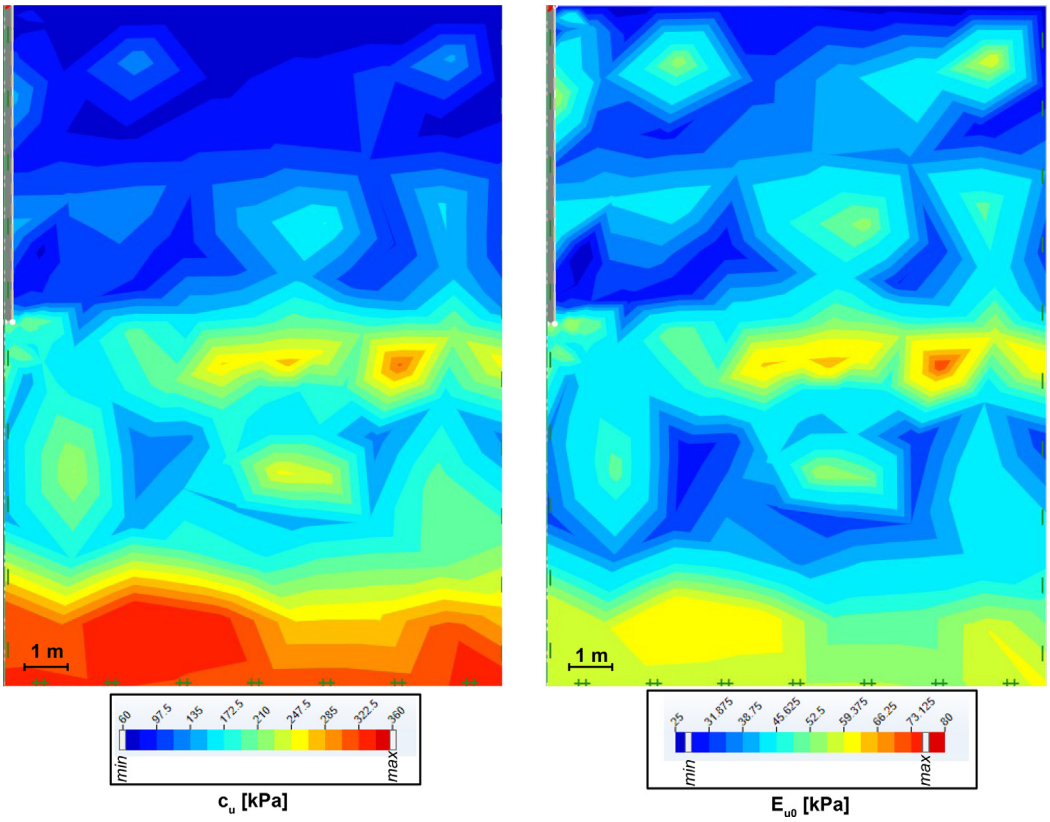

Fig. 15. Strength parameters variability in intact soil in probabilistic analysis (100th run).

MOST WIEDZY Downloaded from mostwiedzy.pl

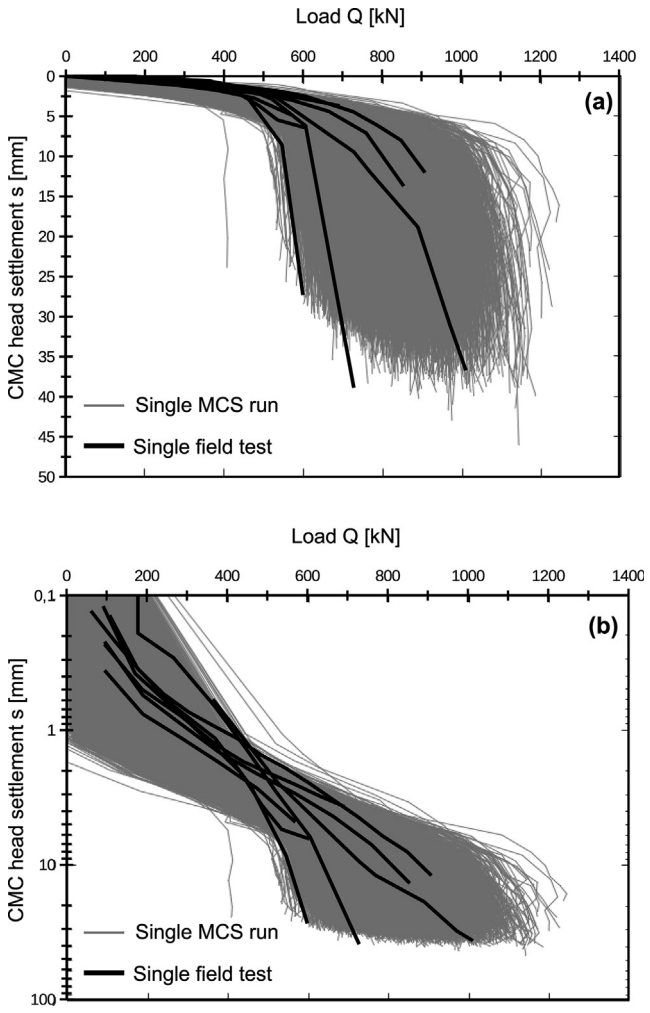

Fig. 16. Q-s curves from SLT and numerical analysis: (a) standard view; (b) log view.

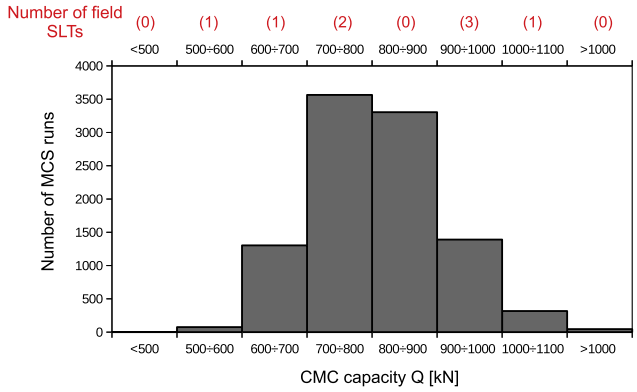

Fig. 17. Probabilistic analysis vs field tests (number of field test in each range of capacities is provided in brackets in the upper part of the figure).

probability of failure is decreasing with number of runs, and $p_f < 1$ % are obtained for n_{sim} greater than 6495, which also fulfills initial assumptions. The standard error decreases from 20kN for $n_{sim} = 100$ to 1.95kN for $n_{sim} = 10\,000$. All mentioned values (COV_{MSC}, SE and p_f) shown good performance of the stochastic CMC model.

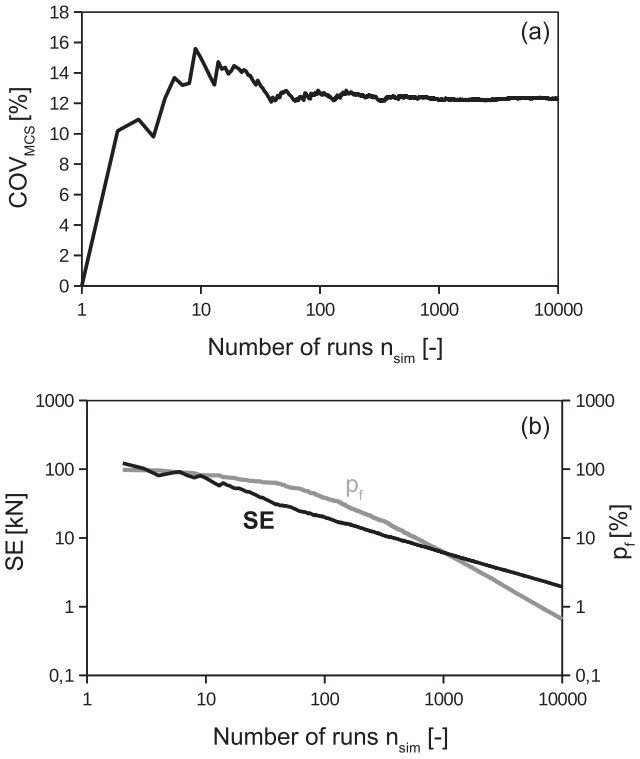

Fig. 18. Distribution of (a) COV_{MSC}, and (b) SE and p_f with number of MSC runs.

5. Conclusions

The presented study allows the following conclusion to be drawn:

1. Inherent variability of soil and interface parameters can successfully explain the variability of SLT results on CMCs in the field.
2. Pile installation usually induces significant overload of the soil, which allows the effective stress approach to estimate failure shear stresses at the interface.
3. It was found that proper incorporation of installation effects is governed by correct estimation of initial stresses and the interface shear strength parameters. This guarantee compatibility with field data. The effective stress approach to determine interface failure shear stress lowers the uncertainty in comparison to CEM estimate.
4. The AUS model captures accurately the nonlinear part of soil and interface behavior and can be successfully used in CMC (or piles) modelling.
5. The variability of basic physical and strength parameters for Poznań clay was estimated and their spatial distribution was directly determined from the lab and field testing and used in the probabilistic modelling of CMC.

Presented paper focused on the practical aspects of statistical analysis of geotechnical data, numerical model development for probabilistic analysis, and results evalua-

MOST WIEDZY Downloaded from mostwiedzy.pl

tion. The good compatibility between probabilistic MCS and field measurement were obtained. The stochastic FEM is thus valuable tool for practitioners and engineers.

Declaration of Competing Interest

The authors declare that they have no known competing financial interests or personal relationships that could have appeared to influence the work reported in this paper.

Acknowledgement

All geotechnical data for Poznań testing site were gathered during realization of the National Center for Research and Development National grant no PBS3/B2/18/2015 and were provided to the author by Menard Sp. z o.o. Author would like to thank Krzysztof Szarf for writing and providing scripts to filter and plot Monte Carlo simulation data, and Lech Bałachowski for proofreading this paper. Author would also like to thank Optum Computational Engineering for providing Academic licence for OptumG2.

References

American Petroleum Institute, 2000. Recommended practice of planning, designing and constructing fixed offshore platforms (No. RP2A), 16th edition. Washington, DC.

ASIRI, 2012. Recommendations for the design, construction and control of rigid inclusion ground improvements.

ASTM D1143, 2020. Standard Test Methods for Deep Foundation Elements Under Static Axial Compressive Load. ASTM International, West Conshohocken, PA.

Au, S., Wang, Y., 2014. Engineering Risk Assessment with Subset Simulation, 1st ed. Wiley. https://doi.org/10.1002/9781118398050

Bałachowski, L., Konkol, J., 2021. Pore water pressure development in soft soil due to installation and loading of controlled modulus columns. J. Geotech. Geoenviron. Eng. 147, 06021014. https://doi.org/10.1061/(ASCE)GT.1943-5606.0002675.

Basu, P., Prezzi, M., Basu, D., 2010. Drilled displacement piles–current practice and design. DFI J.-J. Deep Foundations Inst. 4, 3–20.

Bond, A.J., Jardine, R.J., 1991. Effects of installing displacement piles in a high OCR clay. Géotechnique 41, 341–363. https://doi.org/10.1680/geot.1991.41.3.341.

Brown, D.A., 2005. Practical consideration in the selection and use of continuous flight auger and drilled displacement piles. Geotech. Special Publications, ASCE 129, 251–261.

Brown, D.A., Turner, J.P., Castelli, R.J., 2010. Drilled Shafts: Construction Procedures and LRFD Design Methods (No. FHWA NHI-10-016). National Highway Institute, U.S. Department of Transportation Federal Highway Administration, Washington, DC.

Brown, D.A., Turner, J.P., Castelli, R.J., Loehr, E.J., 2018. Drilled shafts: Construction procedures and design methods (No. FHWA NHI-18-024). National Highway Institute U.S. Department of Transportation Federal Highway Administration, Washington, DC.

Casagrande, A., 1936. The Determination of the Pre-Consolidation Load and Its Practical Significance, in: Proceedings of the 1st International Conference on Soil Mechanics. Presented at the 1st International Conference on Soil Mechanics, Harvard, Harvard, pp. 60–64.

Chen, X., Zhang, J., Xiao, Y., Li, J., 2015. Effect of roughness on shear behavior of red clay–concrete interface in large-scale direct shear tests. Can. Geotech. J. 52, 1122–1135. https://doi.org/10.1139/cgj-2014-0399.

Chin, F.K., 1970. Estimation of the ultimate load of piles not carried to failure, in: Proceedings of 2nd Southeast Asia Conference on Soil Engineering. Presented at the 2nd Southeast Asia Conference on Soil Engineering, Southeast Asian Society of Soil Engineering, Singapore, pp. 81–90.

Cummings, A.E., Kerkhoff, G.O., Peck, R.B., 1950. Effect of driving piles into soft clay. Trans. Am. Soc. Civ. Eng. 115, 275–285.

Czapowski, G., Kasiński, J.R., 2002. Facje i warunki depozycji utworów formacji poznańskiej (in Polish). Prz. Geol. 50, 265–266.

Di Donna, A., Ferrari, A., Laloui, L., 2016. Experimental investigations of the soil–concrete interface: physical mechanisms, cyclic mobilization, and behaviour at different temperatures. Can. Geotech. J. 53, 659–672. https://doi.org/10.1139/cgj-2015-0294.

Doherty, P., Gavin, K., 2011. The shaft capacity of displacement piles in clay: a state of the art review. Geotech. Geol. Eng. 29, 389–410. https://doi.org/10.1007/s10706-010-9389-2.

Dyjor, S., 1970. The Poznań series in west Poland (in Polish with english abstract). Geol. Quarter. 14, 819–835.

Dyjor, S., 1992. Evolution of sedimentation, and process of alterations of sediments in the Poznań suite in Poland (in polish with english abstract). Acta Univ. Wratislav. 26, 3–18.

Fenton, G.A., Griffiths, D.V., 2003. Bearing-capacity prediction of spatially random c ϕ soils. Can. Geotech. J. 40, 54–65. https://doi.org/10.1139/t02-086.

Fenton, G.A., Griffiths, D.V., 2008. Risk Assessment in Geotechnical Engineering. Wiley (John) & Sons, Limited, Hoboken; New Jersey.

Gavin, K., Cadogan, D., Twomey, L., 2008. Axial resistance of CFA piles in Dublin Boulder Clay. Proceedings of the Institution of Civil Engineers - Geotechnical Engineering 161, 171–180. https://doi.org/10.1680/geng.2008.161.4.171.

Griffiths, D.V., Fenton, G.A., 2004. Probabilistic Slope Stability Analysis by Finite Elements. Journal of Geotechnical and Geoenvironmental Engineering 130, 507–518. https://doi.org/10.1061/(ASCE)1090-0241(2004)130:5(507).

Hight, D.W., Leroueil, S., 2003. Characterisation and engineering properties of natural soils, in: Proc. 1st Int. Workshop on Characterisation and Engineering Properties of Natural Soils. Presented at the 1st Int. Workshop on Characterisation and Engineering Properties of Natural Soils, Swets & Zeitlinger, pp. 255–360.

Hird, C. c., Ni, Q., Guymer, I., 2011. Physical modelling of deformations around piling augers in clay. Géotechnique 61, 993–999. https://doi.org/10.1680/geot.9.T.028.

Honjo, Y., Kikuchi, Y., Shirato, M., 2010. Development of the design codes grounded on the performance-based design concept in Japan. Soils Found. 50, 983–1000. https://doi.org/10.3208/sandf.50.983.

Huang, J., Lyamin, A.V., Griffiths, D.V., Krabbenhoft, K., Sloan, S.W., 2013. Quantitative risk assessment of landslide by limit analysis and random fields. Comput. Geotech. 53, 60–67. https://doi.org/10.1016/j.compgeo.2013.04.009.

Karlsrud, K., 2012. Prediction of load-displacement behaviour and capacity of axially loaded piles in clay based on analyses and interpretation of pile load test results, Phd Thesis. ed. Norwegian University of Science and Technology, Trondheim, Norway.

Kawa, M., Puła, W., 2020. 3D bearing capacity probabilistic analyses of footings on spatially variable c–φ soil. Acta Geotech. 15, 1453–1466. https://doi.org/10.1007/s11440-019-00853-3.

Kawa, M., Bagińska, I., Wyjadłowski, M., 2019. Reliability analysis of sheet pile wall in spatially variable soil including CPTu test results. Arch. Civil Mech. Eng. 19, 598–613. https://doi.org/10.1016/j.acme.2018.10.007.

Kawa, M., Puła, W., Truty, A., 2021. Probabilistic analysis of the diaphragm wall using the hardening soil-small (HSs) model. Eng. Struct. 232. https://doi.org/10.1016/j.engstruct.2021.111869 111869.

Komurka, V.E., Wagner, A.B., Edil, T.B, 2003. A Review of Pile Set-Up, in: Proceedings of 51st Annual Geotechnical Engineering Conference. Presented at the 51st Annual Geotechnical Engineering Conference, University of Minnesota, Minnesota, USA, pp. 105–130.

MOST WIEDZY Downloaded from mostwiedzy.pl

Konkol, J., 2017. Numerical analysis of pile installation effects in cohesive soils, PhD Thesis. ed. Gdansk University of Technology, Gdansk.
Kotowski, J., Kraiński, A., 1998. Analiza współczynnika prekonsolidacji w gruntach trzeciorzedowych zaburzonych glacitektonicznie w Łęknicy. Zagadanienia geotechniki środkowego Nadodrza. Zeszyty Naukowe Budownictwo/Politechnika Zielonogórska 115, 81–95.
Krabbenhøft, K., Lymain, A.V., Krabbenhøft, J., 2016. OPTUM G2 - Geotechnical analysis software.
Krabbenhøft, K., Galindo-Torres, S.A., Zhang, X., Krabbenhøft, J., 2019. AUS: anisotropic undrained shear strength model for clays. Int. J. Numer. Anal. Meth. Geomech. 43, 2652–2666. https://doi.org/10.1002/nag.2990.
Krabbenhoft, K., Lyamin, A.V., 2015. Generalised Tresca criterion for undrained total stress analysis. Géotech. Lett. 5, 313–317. https://doi.org/10.1680/jgele.15.00120.
Ku, H.H., 1966. Notes on the use of propagation of error formulas. J. Res. Natl. Bur. Stan. Sect. C. Eng. Instr. 70C, 263–273. https://doi.org/10.6028/jres.070C.025.
Kulhawy, F.H., 1991. Drilled Shaft Foundations. In: Fang, H.-.-Y. (Ed.), Foundation Engineering Handbook. Springer, US, Boston, MA, pp. 537–552. https://doi.org/10.1007/978-1-4757-5271-7_14.
Kulhawy, F.H., Mayne, P.W., 1990. Manual on estimating soil properties for foundation design, Reserch Project 1493-6. Electric Power Research Institute, Palo Alto, California, USA.
Ladd, C.C., 1991. Stability evaluation during staged construction. J. Geotech. Eng. 117, 540–615. https://doi.org/10.1061/(ASCE)0733-9410(1991)117:4(540).
Ladd, C.C., DeGroot, D.J., 2003. Recommended practice for soft ground site characterization: Arthur Casagrande Lecture, in: Proceedings of 12th Panamerican Conference on Soil Mechanics and Geotechnical Engineering. In: Glückauf, M.I.T. (Ed.), Presented at the 12th Panamerican Conference on Soil Mechanics and Geotechnical Engineering, VGE, Verl. Cambridge, Massachusetts, USA, pp. 1–59.
Larisch, M., 2014. Behaviour of stiff, fine-grained soil during the installation of screw auger displacement piles. University of Queensland, Queensland, Australia, PhD Thesis. ed..
Larisch, M., Williams, D.J., Scheuermann, A., McConnell, A., 2014. Stress monitoring using a raked CPTu during screw auger pile installation, in: Proceedings of the 3rd Int. Symposium of Cone Penetration Testing. Presented at the 3rd Int. Symposium of Cone Penetration Testing, TC 102 ISSMGE, Las Vegas, USA, pp. 1–8.
Lehane, B.M., Jardine, R.J., 1994b. Displacement-pile behaviour in a soft marine clay. Canadian Geotechnical Journal 31, 181–191. https://doi.org/0.1139/t94-024.
Lehane, B.M., Jardine, R.J., 1994a. Displacement pile behaviour in glacial clay. Can. Geotech. J. 31, 79–90. https://doi.org/10.1139/t94-009.
Lerche, I., Mudford, B.S., 2005. How many Monte Carlo simulations does one need to do?. Energy Explor. Exploit. 23 405–427. https://doi.org/10.1260/014459805776986876.
Li, X., Cai, G., Liu, S., Puppala, A.J., Zheng, J., Jiang, T., 2019. Undrained shear strength and pore pressure changes due to prestress concrete pile installation in soft clay. Int. J. Civ. Eng. 17, 193–203. https://doi.org/10.1007/s40999-017-0200-0.
Marchetti, S., 1980. In situ tests by flat dilatometer. J. Geotech. Geoenviron. Eng. 106, 299–321.
McCabe, B., Lehane, B.M., 2006. Behavior of axially loaded pile groups driven in clayey silt. J. Geotech. Geoenviron. Eng. 132, 401–410. https://doi.org/10.1061/(ASCE)1090-0241(2006)132:3(401).
Meyerhof, G.G., 1976. Bearing capacity and settlement of pile foundations. J. Geotech. Eng. Div. 102, 197–228. https://doi.org/10.1061/AJGEB6.0000243.
Mitachi, T., Kitago, S., 1976. Change in undrained shear strength characteristics of saturated remolded clay due to swelling. Soils Found. 16, 45–58. https://doi.org/10.3208/sandf1972.16.45.
Mitchell, J.K., Soga, K., 2005. Fundamentals of soil behavior, 3rd ed. Wiley (John) & Sons, Limited, Hoboken; New Jersey.
Mooney, C.Z., 1997. Monte Carlo Simulation. SAGE.
Nguyen, H.H., Khabbaz, H., Fatahi, B., 2017. Effects of installing controlled modulus columns on previously installed columns, in: Proceedings of the 19th International Conference on Soil Mechanics and Geotechnical Engineering. Presented at the 19th International Conference on Soil Mechanics and Geotechnical Engineering, ISSMGE, Seul.
Nguyen, H.H., Khabbaz, H., Fatahi, B., 2019. A numerical comparison of installation sequences of plain concrete rigid inclusions. Comput. Geotech. 105, 1–26. https://doi.org/10.1016/j.compgeo.2018.09.001.
Pestana, J.M., Hunt, C.E., Bray, J.D., 2002. Soil deformation and excess pore pressure field around a closed-ended pile. J. Geotech. Geoenviron. Eng. 128, 1–12. https://doi.org/10.1061/(ASCE)1090-0241(2002)128:1(1).
Pfeiffer, H., Van Impe, W.F., 1993. Evaluation of pile performance based on soil stress measurements: Field test program, in: Proc., 2nd Int. Geotechnical Seminar Deep Foundation on Bored and Auger Piles–BAP II. Presented at the 2nd Int. Geotechnical Seminar Deep Foundation on Bored and Auger Piles–BAP II, Balkema, Amsterdam, Netherlands, pp. 385–389.
Phoon, K.-K., Kulhawy, F.H., 1996. On Quantifying Inherent Soil Variability, in: GSP Geotechnical Special Publication (GSP). Presented at the Uncertainty in the Geologic Environment: from Theory to Practice, American Society of Civil Engineers, New York, NY, Madison, Wisconsin, United States, pp. 326–340.
Phoon, K.-K., Kulhawy, F.H., 1999. Characterization of geotechnical variability. Can. Geotech. J. 36, 612–624. https://doi.org/10.1139/t99-038.
Puła, W., Różański, A., 2012. Reliability of rigid piles subjected to lateral loads. Archiv. Civ. Mech. Eng. 12, 205–218. https://doi.org/10.1016/j.acme.2012.04.007.
Randolph, M.F., Carter, J.P., Wroth, C.P., 1979. Driven piles in clay-the effects of installation and subsequent consolidation. Géotechnique 29, 361–393. https://doi.org/10.1680/geot.1979.29.4.361.
Reddy, S.C., Stuedlein, A.W., 2017. Ultimate limit state reliability-based design of augered cast-in-place piles considering lower-bound capacities. Can. Geotech. J. 54, 1693–1703. https://doi.org/10.1139/cgj-2016-0145.
Slatter, J.W., 2000. The fundamental behaviour of displacement screw piling augers, PhD Thesis. ed. Monash University, Melbourne, Australia.
Spry, M.J., Kulhawy, F.H., Grigoriu, M.D., 1988. In: Reliability-based foundation design for transmission line structures: Geotechnical site characterization strategy, No. EL-5507. Electric Power Research Institute, Palo Alto, CA.
Stróżyk, J., 2015. The overconsolidation ratio of the Poznań clays from the area of SW Poland. Procedia Earth Planet. Sci., World Multidiscip. Earth Sci. Sympos., WMESS 2015 (15), 293–298. https://doi.org/10.1016/j.proeps.2015.08.071.
Stróżyk, J., Tankiewicz, M., 2016. The elastic undrained modulus E for stiff consolidated clays related to the concept of stress history and normalized soil properties. Studia Geotech. Mech. 38, 67–72. https://doi.org/10.1515/sgem-2016-0025.
Stuedlein, A.W., Neely, W.J., Gurtowski, T.M., 2012. Reliability-based design of augered cast-in-place piles in granular soils. J. Geotech. Geoenviron. Eng. 138, 709–717. https://doi.org/10.1061/(ASCE)GT.1943-5606.0000635.
Suleiman, M.T., Ni, L., Davis, C., Lin, H., Xiao, S., 2015. Installation effects of controlled modulus column ground improvement piles on surrounding soil. J. Geotech. Geoenviron. Eng. 142, 04015059. https://doi.org/10.1061/(ASCE)GT.1943-5606.0001384.
Tang, C., Phoon, K.-K., 2018. Statistics of model factors in reliability-based design of axially loaded driven piles in sand. Can. Geotech. J. 55, 1592–1610. https://doi.org/10.1139/cgj-2017-0542.
Tomlinson, M., Woodward, J., 2015. Pile Design and Construction Practice, Sixth, Edition. ed. CRC Press, New York.
Uzielli, M., Lacasse, F., Nadim, F., Phoon, K.-K., 2006. Soil variability analysis for geotechncial practice, in: Proc. 2nd Int. Workshop Characterization and Engineering Properties of Natural Soils. Pre-

MOST WIEDZY Downloaded from mostwiedzy.pl

sented at the 2nd Int. Workshop "Characterization and Engineering Properties of Natural Soils," Taylor & Francis Group, Singapore, pp. 1653–1752.

VanMarcke, E., 1983. Random Fields: Analysis and Synthesis, Web Edition by Rare Book, Services. ed. MIT Press, Cambridge MA.

Wang, Y., Cao, Z., 2013. Expanded reliability-based design of piles in spatially variable soil using efficient Monte Carlo simulations. Soils Found. 53, 820–834. https://doi.org/10.1016/j.sandf.2013.10.002.

Wang, Y., Cao, Z., 2015. Practical reliability analysis and design by Monte Carlo Simulation in spreadsheet. Risk and Reliability in Geotechnical Engineering. CRC Press.

Wendel, E., 1900. On the test loading of piles and its application to foundation problems in Gothenburg. Tekniska Samfundets Handlingar, 3–62.

Won, J.Y., 2013. Anisotropic Strength Ratio and Plasticity Index of Natural Clays, in: Roceedings of the 18th International Conference on Soil Mechanics and Geotechnical Engineering. Presented at the 18th International Conference on Soil Mechanics and Geotechnical Engineering, ISSMGE, Paris, France, pp. 445–448.

Xu, X.T., Liu, H.L., Lehane, B.M., 2006. Pipe pile installation effects in soft clay. Proceedings of the Institution of Civil Engineers-Geotechnical Engineering 159, 285–296. https://doi.org/10.1680/geng.2006.159.4.285.

Yang, L., Liang, R., 2006. Incorporating set-up into reliability-based design of driven piles in clay. Can. Geotech. J. 43, 946–955. https://doi.org/10.1139/t06-054.

Yannie, J., 2012. Change of shear strength in soft soil excavations. Presented at the EYGEC 2012 - setting the scene for future European geotechnical research, Gothenburg, Sweden, pp. 113–118.

Zapata-Medina, D.G., Finno, R.J., Vega-Posada, C.A., 2014. Stress history and sampling disturbance effects on monotonic and cyclic responses of overconsolidated Bootlegger Cove clays. Can. Geotech. J. 51, 599–609. https://doi.org/10.1139/cgj-2013-0292.

Zhang, J., Tang, W.H., Zhang, L.M., Huang, H.W., 2012. Characterising geotechnical model uncertainty by hybrid Markov Chain Monte Carlo simulation. Comput. Geotech. 43, 26–36. https://doi.org/10.1016/j.compgeo.2012.02.002.

Zhu, J.-G., Yin, J.-H., 2000. Strain-rate-dependent stress-strain behavior of overconsolidated Hong Kong marine clay. Can. Geotech. J. 37, 1272–1282. https://doi.org/10.1139/t00-054.

MOST WIEDZY Downloaded from mostwiedzy.pl